Spin–orbit effects on the structural, homotop, and magnetic configurations of small pure and Fe-doped Pt clusters

ARTICLE *in* JOURNAL OF NANOPARTICLE RESEARCH · JANUARY 2014

Impact Factor: 2.18 · DOI: 10.1007/s11051-013-2222-0

4 AUTHORS:

F. Aguilera-Granja
Universidad Autónoma de San Luis Po…
150 PUBLICATIONS **1,368** CITATIONS
SEE PROFILE

Pedro Gilberto Alvarado-Leyva
Universidad de Valladolid
19 PUBLICATIONS **16** CITATIONS
SEE PROFILE

A. Garcia-Fuente
University of Oviedo
21 PUBLICATIONS **165** CITATIONS
SEE PROFILE

Andrés Vega
Universidad de Valladolid
175 PUBLICATIONS **1,950** CITATIONS
SEE PROFILE

J Nanopart Res (2014) 16:2222
DOI 10.1007/s11051-013-2222-0

RESEARCH PAPER

Spin–orbit effects on the structural, homotop, and magnetic configurations of small pure and Fe-doped Pt clusters

P. G. Alvarado-Leyva · F. Aguilera-Granja · A. García-Fuente · A. Vega

Received: 7 February 2013 / Accepted: 18 December 2013

Abstract We report ab initio calculations of the atomic and electronic structures, and related magnetic properties of platinum clusters of seven atoms both pure and substitutionally doped with an iron impurity. A relativistic Hamiltonian including spin–orbit coupling effects is self-consistently solved in the noncollinear framework within the density functional theory as implemented in the VASP code. We show that spin–orbit coupling is crucial for determining the energetic order of structural isomers of small platinum clusters, but not for the low-lying iron-doped platinum clusters. We analyze the influence of Fe doping on the overall improvement of the magnetic efficiency of the nanoparticle, i.e., large total moment and high stability against remagnetization. Results are reported for the spin–orbit energy, the magnetic anisotropy energy corresponding to the remagnetization barrier, and the orbital contribution to the total magnetic moment, which can be experimentally measured in free-standing clusters by means of X-ray magnetic circular dichroism spectroscopy.

Keywords Transition-metal clusters · Geometrical properties · Magnetic properties · Electronic properties · DFT methods · Magnetic anisotropy · Modeling and simulation

Introduction

The magnetic properties of clusters of transition metal (TM) atoms have been for a long time the subject of intense research with the aim of understanding how magnetism changes, when the dimension of a material is reduced to the nanometer length scale and quantum confinement effects come into play, but also with a view to the potential technological applications, such as the design of high-density magnetic storage devices.

Magnetism, as a collective phenomenon, depends on many factors involving the electronic, as well as the ionic degrees of freedom, and for its full description, at the quantum-mechanical level, both the orbital and the spin spaces of states have to be considered. However, certain approximations have been done with success in the most previous studies of small clusters which

P. G. Alvarado-Leyva
Facultad de Ciencias, Universidad Autónoma de San Luis Potosí, 78000 San Luis Potosí, Mexico

F. Aguilera-Granja
Instituto de Física "Manuel Sandoval Vallarta", Universidad Autónoma de San Luis Potosí, 78000 San Luis Potosí, Mexico

F. Aguilera-Granja
Donostia International Physics Center (DIPC), 20018 San Sebastián, Spain

A. García-Fuente (✉) · A. Vega
Departamento de Física Teórica, Atómica y Óptica, Universidad de Valladolid, 47011 Valladolid, Spain
e-mail: amador.uva@gmail.com

Published online: 12 January 2014

allowed to extract important general trends with the available computational resources. For instance, the enhancement of the magnetic moment in ferromagnetic clusters as compared to the bulk, associated with the narrowing of the *d*-band due to loss of coordination was predicted long time ago on the basis of simple tight-binding models and without relaxing the atomic structures (Vega et al.1993). This general trend can be qualitatively rationalized in terms of the average atomic coordination and the average interatomic distances without the need of an accurate determination of the geometrical shape. Another example is the consideration of the same spin-quantization axis for the whole cluster that is a good approximation for the late 3*d* TM clusters, as well as for the 4*d* and 5*d* ones in which magnetic frustration and noncollinear magnetic ordering rarely take place. Another example is the restriction to the spin space of states in scalar-relativistic calculations, thus neglecting the orbital contribution and the spin–orbit coupling (SOC) when estimating the total magnetic moment of 3*d* TM clusters. This is a good approximation because, although the isolated atoms with open shells have noticeable spin and orbital magnetic moments (Hund's rule), the orbital ones are quenched in the bulk by the symmetry of the crystal, and also, to a large extent, when forming small clusters. Moreover, spin–orbit interaction is rather weak in *3d* systems (Fritsch et al. 2008; Błoński and Hafner 2009, 2011; Sahoo et al. 2010).

A more detailed understanding of the magnetic behavior of TM clusters, comprising for instance possible spin excitations (spin isomers), magnetostrictive effects, structure-related magnetic magic numbers, or magnetic anisotropy, requires a more accurate description in which constrictions on the structural shape, on the spin-quantization axis, or on the spin space of states have to be released. Although corresponding accurate descriptions are feasible nowadays in the framework of the density functional theory (DFT) as implemented in several codes, studies considering some of the above issues are still scarce, an example being the full inclusion of the SOC which implies also to treat noncollinear magnetism.

From the technological point of view, one of the main issues is the fabrication of high-performance magnetic storage devices, whose main component is the magnetic bit. With the aim to increase the magnetic storage density, the bit should be as small as possible, it should have a large total magnetic moment and a large magnetic anisotropy energy (MAE) to avoid loss of information due to magnetization reversal. Magnetic clusters are good candidates for these purposes (Sun et al. 2000). Small clusters of the 3*d* ferromagnetic TM elements Fe, Co, and Ni, have been shown to exhibit parallel magnetic coupling, reminiscent from their bulk ferromagnetism, but with the enhanced magnetic moments due to their finite size, and forming a monodomain (Bucher et al. 1991; Billas et al. 1994; Apsel et al. 1996; Knickelbein 2001; Castro et al. 1997; Diéguez et al. 2001). However, 3*d* clusters have very small MAE (Fritsch et al. 2008; Błoński and Hafner 2009 and 2011; Sahoo et al. 2010) despite their reduced symmetry compared to the bulk, and the weak SOC of their atoms. In order to find TM clusters with large MAE one has to look for those formed by elements with strong SOC. It has been recently shown that 5*d* TM clusters, particularly those made of Pt atoms fulfill this requirement (Huda et al. 2006; Fernández-Seivane and Ferrer 2007; Błoński et al. 2011). In fact, for small Pt clusters (up to six atoms), the SOC can be a driving force for determining the atomic structure and the energetic order of structural isomers. Moreover, SOC leads to a large contribution of the orbital moment due to the total magnetic moment of the Pt clusters.

Although less extensive than in the single-component case, investigation on the magnetic behavior of TM bimetallic clusters has also been performed (Toneguzzo et al. 1998; Zitoun et al. 2002; Polak and Rubinovich 2004; Zhen et al. 2008; Meshcheryakov et al. 2008; García-Fuente et al. 2009). Mixing elements to form a heteroatomic cluster (the nanometric equivalent to alloying or to doping in the dilute limit of impurities), opens the possibility to tailor the magnetic properties through the choice of the component species and the composition, often leading to the new magnetic states that are not possible in homonuclear TM clusters. Chemical order comes into play now, as well as possible electronic cooperative effects. Although a big effort is being made in the investigation of magnetic heteroatomic clusters (Toneguzzo et al. 1998; Zitoun et al. 2002; Polak and Rubinovich 2004; Zhen et al. 2008; Meshcheryakov et al. 2008; García-Fuente et al. 2009), SOC effects have not been investigated so far for these systems. Up to which extent the SOC is a driving force for determining the

structure, the most stable homotop of a given mixed cluster, the energetic order of isomers, as well as the corresponding magnetic state, still remain open questions. Fe-doped Pt clusters are very interesting in this context, since they combine the large MAE of Pt clusters with the large magnetic moment of the Fe atom.

In the present work, we perform a systematic study of the structural and magnetic properties of the seven atom clusters made of pure Pt (Pt_7), as well as with a substitutional impurity of Fe (Pt_6Fe). At the DFT level, we determine the low-lying structural isomers and homotops, together with their magnetic states, including the SOC contribution. We find the easy axis for magnetization, the SOC energy, and the MAE which corresponds to the energy barrier for remagnetization. We analyze the influence of Fe doping on the overall improvement of the magnetic efficiency of the nanoparticle, i.e., large total moment and high stability against remagnetization. By comparing with the scalar-relativistic calculations, we discuss how SOC influences the chemical order of these dilute bimetallic molecular magnets. We also calculate the orbital contribution to the total magnetic moment, which can be experimentally measured by means of X-ray magnetic circular dichroism spectroscopy of size-selected clusters (Peredkov et al. 2011; Niemeyer et al. 2012).

The seven atoms platinum cluster is chosen for the present study because it is small enough for the SOC effect to be significant, while it is large enough to present a variety of plausible structures, many of which have been proposed in previous works (Kumar and Kawazoe 2008; Montejano-Carrizales et al. 2011). Those geometrical arrangements plus some variants are considered as input in the present study for determining a set of low-lying structural isomers both with the scalar-relativistic treatment as well as including the SOC effect.

The rest of the paper is organized as follows. The technical details of the computational method used are described in "Details of the computational procedure" section. In "Scalar-relativistic calculations" section, we present the results obtained for the pure and Fe-doped Pt heptamer in the scalar-relativistic calculations. "Spin–orbit coupling effects" section is devoted to discuss the effects of SOC. We summarize our main conclusions in the "Summary and conclusions" section.

Details of the computational procedure

Our fully self-consistent DFT calculations were performed using the plane-wave code VASP (Kresse and Hafner 1993; Kresse and Furthmuller 1996), which solves the spin-polarized Kohn–Sham equations within the projector-augmented wave (PAW) approach. This approach leads to the exact all-electron potential and allows a considerable efficiency in terms of computational time. For the exchange and correlation potential we used the Perdew–Burke–Ernzerhof form of the generalized gradient approximation (Perdew et al. 1996). A Hamiltonian containing all relativistic corrections up to the second order in the fine-structure constant (Kresse and Lebacq 2013) is solved in the noncollinear approximation (Hobbs et al. 2000; Marsman and Hafner 2002). The plane-wave basis set was extended up to an energy cutoff of 300 eV, and we used an energy criterium of 10^{-6} eV for converging the electronic part. Since the MAE is expected to be of the order of meV in Pt, care has to be taken as regard to the convergence criteria. Tests performed, in selected cases, with a bigger energy cutoff for plane waves (up to 600 eV) and with a finer criterium for the electronic part (down to 10^{-9} eV) gave virtually the same results when SOC was considered.

Local electronic charge and local magnetic moments distribution are quantities which are usually difficult to define. They can be determined by projecting the plane wave components onto spherical waves inside overlapping spheres. However, this approach depends on the atomic radii of the overlapping spheres and the resulting sum of local charges and moments is not, in general, equal to the total charge and total magnetic moment, respectively, obtained though VASP. In order to overcome this issue, we have evaluated these local quantities using Bader's method (Bader 1990). Bader's method divides the cluster in atomic volumes by locating the zero-flux surfaces of the electron density field. Using this method, the sum of the local charges and moments recovers the total electronic charge and magnetic moment. Nevertheless, We have verified that Bader's distribution of local quantities preserves in a large extent that the relative proportions given by the projection of plane waves.

In the calculations, the clusters were placed in a cubic supercell of size $20 \times 20 \times 20$ $Å^3$, large enough to neglect the interaction between the cluster

and its replicas in neighboring cells, and to consider only the Γ point ($k = 0$) when integrating over the Brillouin zone.

A large number of atomic configurations were considered as follows: (i) open structures based on the planar cubic motifs, (ii) atomic structures reported in the literature for 7-atoms clusters, and (iii) structures designed by adding (subtracting) a single atom to (from) the lowest energy structures previously reported for 6- (8-)atom clusters. A large number of different magnetic configurations were also calculated for every cluster structure with the aim of finding its corresponding lowest energy spin isomer. All the structures were relaxed without any symmetry or spin constraints until interatomic forces were smaller than 0.005 eV/Å. In the case of the Fe-doped Pt clusters, we analyzed all possible homotops of each structure, i.e., all the possible locations of the Fe atom among the sites of the cluster, and as in the pure Pt clusters, all the spin isomers in the scalar-relativistic calculations that we performed in a first step. In a second step, we switched on the SOC interaction. At this point, in order to find the easy axis and the hard axis for magnetization, we had to perform for each structure/homotop a set of SOC-calculations for different initial orientations of the magnetic moments by selecting the different possible spin-quantization axes taking advantage of the spatial symmetry properties of the cluster. We further relaxed the structure to account for the influence of the SOC on the structural properties. The difference between the total energy obtained with SOC in the easy axis and the total energy obtained in the scalar-relativistic calculation for a given cluster gives the SOC energy. The difference between the total energy obtained for the easy axis and that obtained for the hard axis corresponds to the MAE, and it is an estimation of the energy barrier for remagnetization. The binding energies of the clusters were computed as the sign-reversed total energies relative to the same number of isolated atoms and normalized per atom.

Scalar-relativistic calculations

Platinum heptamer

The results of the scalar-relativistic calculations for the pure Pt_7 cluster are summarized in Fig. 1. Both the ground state and the first three isomers have a two-dimensional planar structure. The ground state is based on square motifs and has a total spin moment of 4 μ_B corresponding to a quintet spin state. This structure has also been reported in previous works (Kumar and Kawazoe 2008; Montejano-Carrizales et al. 2011). The first isomer is a spin isomer (triplet spin state) of this same structure, and it is less stable than the ground state by only 10 meV/atom. The next two isomers have the hexagonal symmetry but different spin states, quintet and triplet respectively. These structures were not reported previously in the literature. The higher energy isomers have three-dimensional structures based, most of them, on pyramidal motifs. We note that some of these structural arrangements were not reported in previous works, and that although we have done an exhaustive search, we can not guarantee to have found all the most stable isomers. A general trend is the ferromagnetic-like coupling obtained in all the low-lying isomers of Pt_7. Several spin isomers of the three-dimensional prism based structure are also present at higher total-energy differences with respect to the ground state. A different spin state is generally accompanied by a structural distortion due to electron redistribution. For instance, the eleventh isomer with a total spin moment of 8 μ_B has a more prolate structure than the fifth one with 4 μ_B.

Iron-doped platinum heptamer

Doping the Pt cluster with a substitutional Fe impurity has the dramatic effects on both the structure and spin state. Figure 2 illustrates the most stable isomers of the Pt_6Fe cluster resulting from the scalar-relativistic calculations. Three-dimensional structures are now clearly favored over the planar ones (not shown in the figure) which appear only at quite higher energies above the three-dimensional ground state. The geometry of the ground state can be seen as an hexahedron (or triangular bipyramid) plus two capping atoms, one on a hollow site and the other on a bridge site. This symmetry is the same as that of the seventh isomer reported in Fig. 1 for the pure Pt_7 cluster. In the pure case, this structure is at about 35 meV/atom above the ground state. Therefore, the structural trends completely change upon the substitution of a single Pt atom by Fe. Among the next low-lying isomers, one can identify other symmetries present in some of the

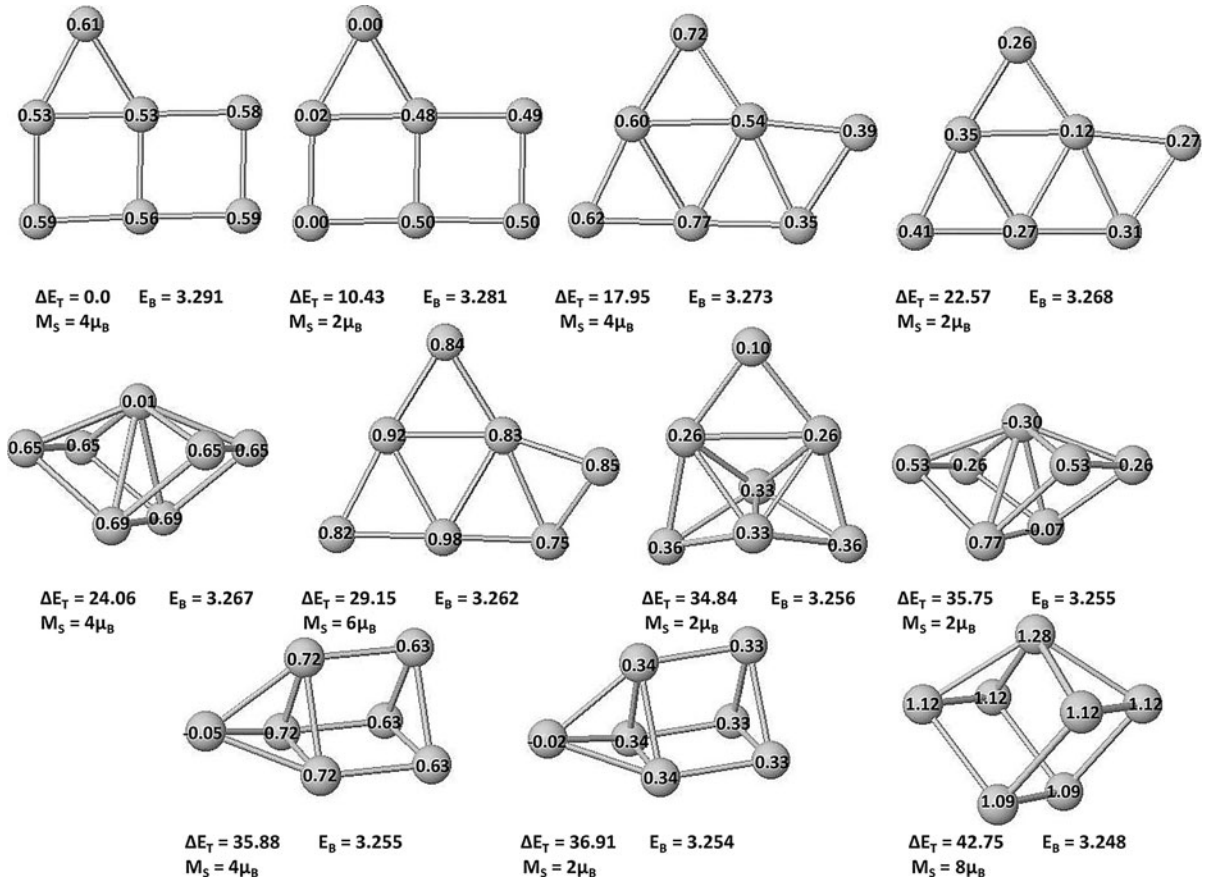

Fig. 1 Lowest-energy isomers of Pt_7 as obtained in the scalar-relativistic calculation. ΔE_T is the total energy per atom relative to the ground state, in units of meV; E_B is the binding energy per atom, in units of eV. M_S is the total spin magnetic moment

three-dimensional isomers found in the pure case. Doping with Fe does not modify, in general, the parallel coupling between the local spin magnetic moments, thus yielding a ferromagnetic-like arrangement in the ground state and in the most low-lying isomers. Exception of this rule are the fifth and seventh low-lying isomers in which some antiparallel couplings exist together with the quenched local moments in certain Pt atoms, giving rise to a total moment of 4 and 2 μ_B, respectively. Antiferromagnetic spin isomers other than those have been only found at much higher energy differences with respect to the ground state, indicating that such a low moment spin isomers are not energetically favorable in Fe-doped Pt clusters of this size. Since, the above mentioned cases are different spin isomers of the ground state homotop, we performed a crosscheck for this cluster using a different implementation of the DFT, namely the code SIESTA (Soler et al. 2002), with the same approximation for the exchange and correlation potential, the same accuracy parameters for the structural relaxation, convergence of the electronic part, and electronic temperature as with VASP. More details of the basis and pseudopotentials used with SIESTA can be seen in a previous work (Aguilera-Granja et al. 2010). SIESTA reproduces exactly the same map of spin isomers as VASP for the ground state structure, with the minimum energy in the nonet state (total moment of 8 μ_B) and the same antiferromagnetic-like couplings in the spin isomers with 4 and 2 μ_B. Therefore, doping with Fe increases the total spin moment of the ground state by a factor of two as compared with the planar ground state of the pure case, and by a factor of four if we compare with the most stable of the pure clusters with the same three-dimensional structure (seventh isomer in Fig. 1). This increase of the total moment is due to the contribution of the Fe impurity with a local spin moment of 3.54 μ_B

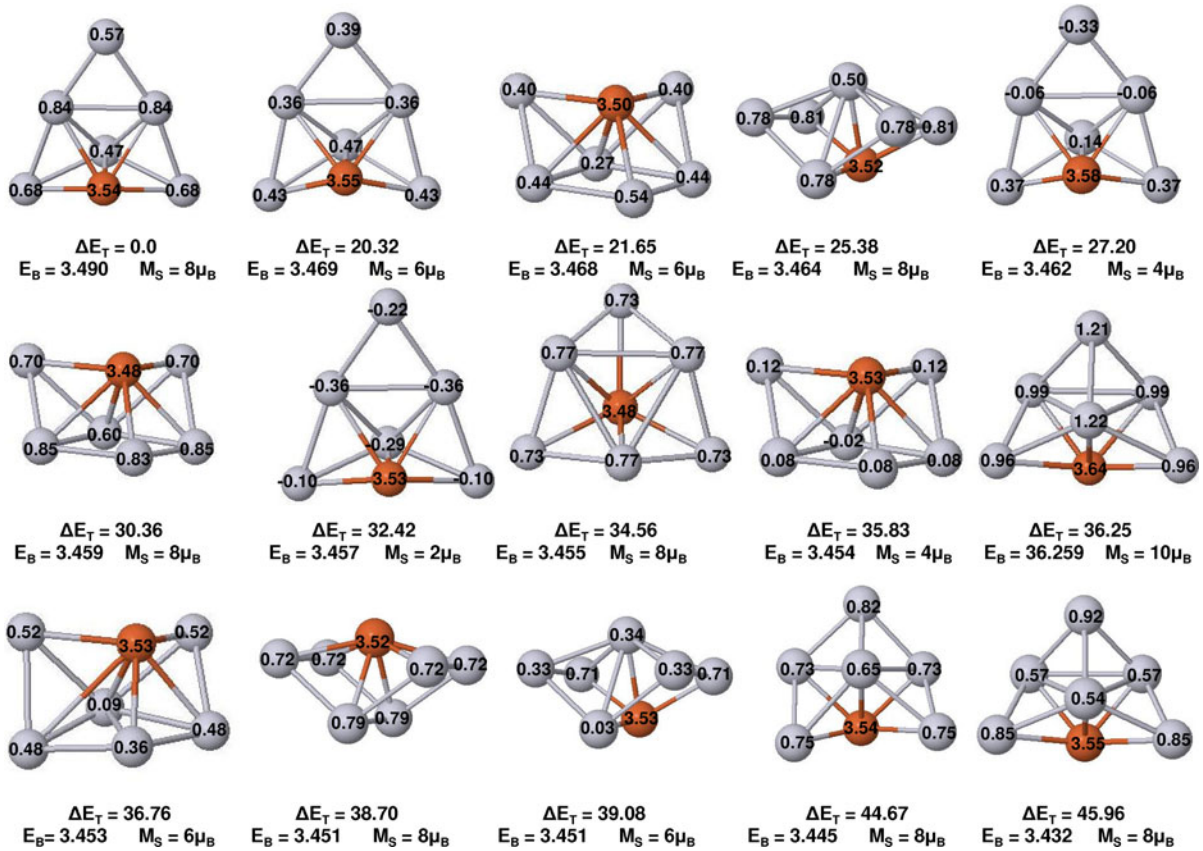

Fig. 2 (Color online) Lowest-energy isomers of Pt_6Fe as obtained in the scalar-relativistic calculation. ΔE_T is the total energy per atom relative to the ground state, in units of meV; E_B is the binding energy per atom, in units of eV. M_S is the total spin magnetic moment

together with the increase of the magnetic moment induced on the Pt atoms. This also happens in other isomers (compare the local moments of the most stable isomers corresponding to a given family in Fig. 1). Therefore, the overall effect of doping with Fe, from the magnetic point of view, is to increase the total moment and, thus, to improve the magnetic efficiency of the nanoparticle in this respect. Several spin isomers corresponding to structures different from the ground state one and to a given homotop of the same structure can be also identified. The energy difference between spin isomers or between homotops is of the same order of magnitude, For instance, the 3rd, 6th, and 9th low-lying isomers are spin isomers (spin moment of 6, 8, and 4 μ_B, respectively) of the same homotop of a square pyramid plus two capping atoms (21.7, 30.4, and 35.8 meV/atom higher in energy than the ground state). The 12th low-lying isomer is a different homotop of the 4th low-lying isomer, both having the same spin state of 8 μ_B. These two are separated by 13.3 meV/atom. Therefore, spin isomers and homotops, or in other words spin excitations and chemical order compete within the same energy window. Doping with Fe thus leads to a very rich variety of isomers of the different kinds. A comparison of the local spin magnetic moment distribution of different spin isomers of the same homotop (see the examples just mentioned in Fig. 2) indicates that the different spin state is essentially due to the exchange splitting of the Pt atoms. The local magnetic moment of the Fe atom is nearly unchanged. Another important finding is that upon substitutional doping with Fe, binding energies increase about 175 meV/atom which means that the Fe impurity helps in stabilizing the nanoparticle besides increasing its total magnetic moment, both facts being relevant from the technological point of view.

Spin–orbit coupling effects

In the case of the pure Pt heptamer, a planar structure is also the most stable atomic arrangement when SOC is taken into account, as illustrated in Fig. 3. Note that the spin space of states is connected with the orbital space of states through the SOC interaction. Therefore, an absolute orientation of the spin and orbital magnetic moments with respect to the cluster geometry exists now, in contrast to the scalar-relativistic approach discussed in the previous section. Blue and black arrows in Fig. 3 (and later in Fig. 4) correspond to the spin and orbital contribution to the local magnetic moments and their orientation corresponds, in average, either to the easy axis of magnetization of the cluster or to the hard axis, as indicated in the figure. The energy difference between both configurations is the magnetic anisotropy energy that essentially indicates up to which extent the magnetic moment is coupled to the cluster structure, being an estimation of the activation barrier for remagnetization. Previous works showed that the SOC favors planar structures in Pt clusters up to five atoms (Huda et al. 2006; Błoński et al. 2011). In Pt_7 the planar ground state geometry is the same in the absence of SOC, but the SOC modifies the energetic order of the most stable low-lying isomers. The fifth low-lying structure in the absence of SOC results to be the second one with SOC. We note that when considering SOC the binding energy of Pt_7 clusters is reduced compared with the scalar-relativistic calculation, due to the open 5*d* shell of the isolated Pt atoms which gives them a larger total energy when SOC is taken into account. The SOC does not modify significantly the total magnetic moment of the ground state (see Figs. 1, 3). However, it is interesting to point out that the spin contribution (2.64 μ_B) is comparable to the orbital one (1.87 μ_B) and considerably smaller than the spin moment obtained in the scalar-relativistic calculation. We find a similar trend as that obtained by Błoński and Hafner (2011) in Ni clusters, that is the SOC leads to a mixing of the spin states of low-energy spin isomers obtained in the scalar-relativistic calculation. For instance, we recall that the second isomer of Fig. 1 has the same structure as the ground state, but a spin moment of 2 μ_B. The spin contribution to the total moment when considering the SOC (2.64 μ_B) is in between this value and the 4 μ_B of the ground state. Orbital moments are collinear with the spin ones in the ground state, but not in the first low-lying isomer. Both the spin and orbital moments are strongly quenched in the ground state planar arrangement if forced to point in the direction of the hard axis which is the out-of-plane direction (see Fig. 3). This contributes to the relatively large MAE (40 meV) obtained in the ground state. In the metastable isomers the moment quenching in the hard axis is not a general trend (see Fig. 3). The orbital and spin contributions to the total moment can be measured at present through XMCD. Therefore, our predictions can be experimentally verified. Due to the small size of these clusters, we expect the local magnetic moments of all the atoms to be part of the same magnetic domain. Thus, all the local magnetic moments are expected to rotate together in a remagnetization event, which means one degree of freedom associated with such process. Therefore, we can expect these magnetic configurations to be stable against magnetization reversal by thermal excitation at room temperature if the MAE is higher than K_BT (25 meV). Also, for temperatures with corresponding energies below the MAE, we can consider the cluster as a rigid rotor, since the magnetic moment is strongly coupled to the easy axis, meanwhile beyond this energy it would be fluxional. This analysis has important implications for interpreting Stern–Gerlach experiments performed at a given temperature.

As regards the SOC effect on the binary clusters Pt_6Fe resulting upon doping, we find most of the above mentioned trends. However, in this case the energetic order of the most stable low-lying structural isomers are the same as without SOC. Figure 4 displays the three most stable low-lying isomers. From the structural point of view, only local relaxation effects are noticeable as compared with Fig. 2. As in the pure platinum clusters, the SOC leads here also to a mixing of the spin states of low-energy spin isomers obtained in the scalar-relativistic calculation. For instance, the spin contribution to the moment of the ground state (5.17 μ_B) is in between the spin moment of the second and fifth isomers in Fig. 2. In fact, it can be seen as a mix of the spin isomers found without SOC for this structure. With the addition of the orbital contribution which amounts to near 1 μ_B, the ground state reaches a total moment of nearly 6 μ_B, resulting lower than in the scalar-relativistic calculation although still higher that in the pure Pt_7 cluster. The MAE in the ground state amounts to 24 meV, slightly lower that in the pure Pt_7 (40 meV). In this respect, the planar geometry of Pt_7 is

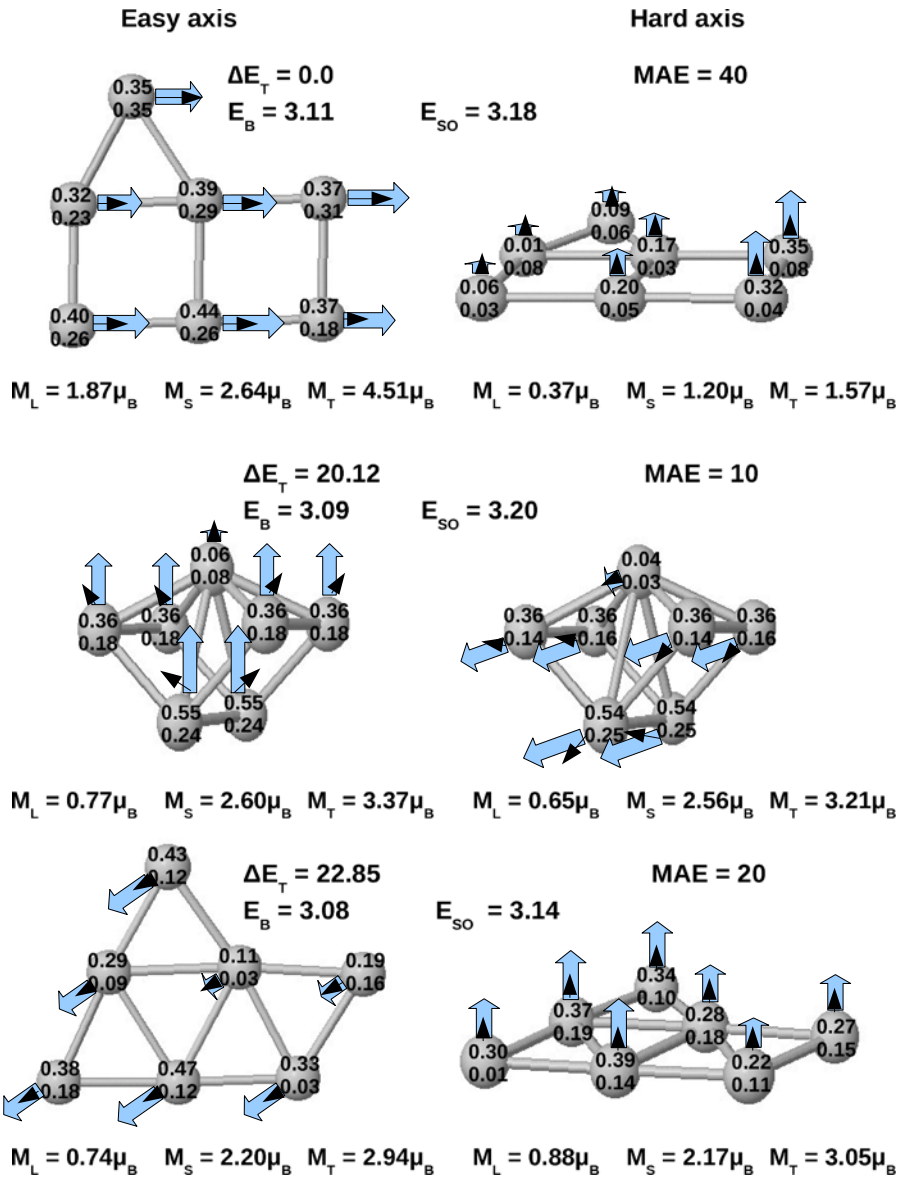

Fig. 3 (Color online) The three lowest-energy isomers for Pt_7 as obtained when SOC is taken into account. *Blue* (*black*) *arrows* are used to represent the spin (orbital) magnetic moments on each atom. The *left* (*right*) *side* corresponds to the easy (hard) axis configuration. ΔE_T is the total energy per atom relative to the ground state, in units of meV; E_B is the binding energy per atom, in units of eV; E_{SO} is the spin–orbit energy, in units of eV; the magnetic anisotropy energy (MAE) is given in meV. Below each cluster configuration are given the orbital (M_L) and the spin (M_S) contributions to the total magnetic moment (M_T)

expected to induce itself a larger MAE. However, it is interesting to note that for certain metastable isomers that have a similar atomic arrangement in both the pure and mixed cases, doping with Fe not only enhances the total moment of the cluster as discussed in the previous section but also contributes to increasing the MAE. An example of this fact that is the third isomer of Fig. 4 with a MAE of about 18 meV, which can be compared with its pure counterpart, that is the second isomer of Fig. 3 (MAE of 10 meV). The quite large magnetic moment of Fe can be at the origin of this trend, since more energy is

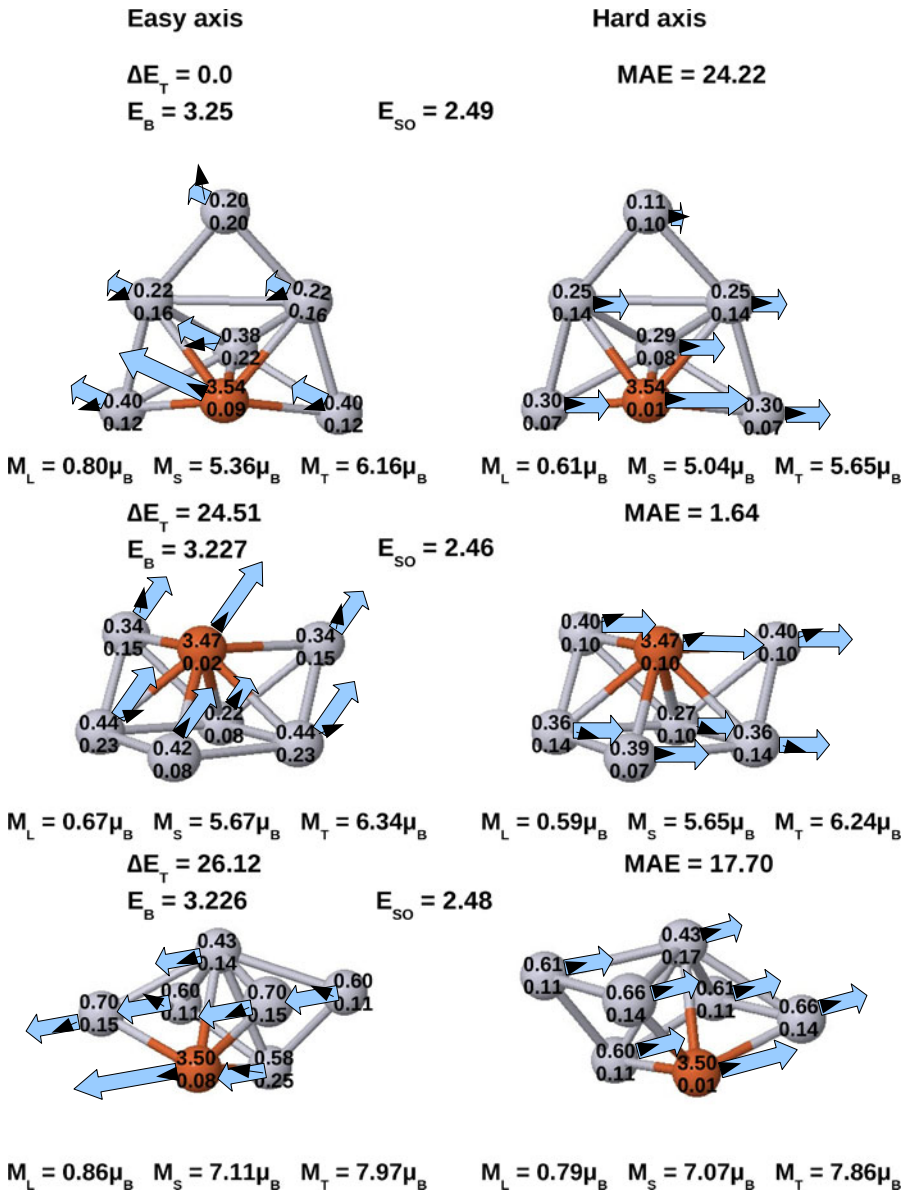

Fig. 4 (Color online) The three lowest-energy isomers for Pt_6Fe as obtained when SOC is taken into account. *Blue* (*black*) *arrows* are used to represent the spin (orbital) magnetic moments on each atom. The *left* (*right*) *hand side* corresponds to the easy (hard) axis configuration. ΔE_T is the total energy per atom relative to the ground state, in units of meV; E_B is the binding energy per atom, in units of eV; E_{SO} is the spin–orbit energy, in units of eV; the magnetic anisotropy energy (MAE) is given in meV. Below each cluster configuration are given the orbital (M_L) and the spin (M_S) contributions to the total magnetic moment (M_T)

required to rotate a large magnetic moment from an easy axis to a hard axis than a small moment. In other words, the SOC effect not only increases the atomic number of the element (relativistic effects become more important) but also increases the spin magnetic moment, which becomes more difficult to rotate. This trend is interesting since for certain atomic configurations, doping with iron improves the quality of the magnetic nanoparticle in three aspects of technological relevance: increase of the total magnetic moment, of the MAE, and of the binding energy as we have seen in the previous section. Of course, with regard to the MAE this result is obtained when doping with a single Fe impurity, but it is expected that as

increasing the relative Fe concentration in a PtFe binary cluster, the MAE decreases since the MAE in pure Fe clusters is much smaller than in pure Pt clusters.

The MAE is expected to be larger, in general, for low dimensional structures, particularly in atomic arrangements with well defined symmetry axes or planes. In order to check if this trend is fulfilled here, we have switched on the SOC also in the 12th isomer of Fig. 2. This isomer is a more symmetrical homotop (symmetry C_{2v}) of the third isomer of Fig. 4 discussed just above and shown to have larger MAE than its pure counterpart. This more symmetrical homotop has a MAE as large as 31 meV, together with a total moment of 9 μ_B (with collinear spin and orbital moments), both values larger than those of the significant isomers previously discussed. Although it is a metastable solution, the obtained results are indicative of a way to design the high-performance of magnetic grains. Considering that these grains are generally supported on substrates, such metastable configurations should be more feasible than in a free-standing environment.

Summary and conclusions

In this work we performed DFT-GGA calculations of the structures, binding energies, magnetic anisotropy energy, and spin and orbital magnetic moments of platinum clusters of seven atoms both pure (Pt_7) and substitutionally doped with an iron impurity (Pt_6Fe) using the code VASP (Kresse and Hafner 1993; Kresse and Furthmuller 1996).

Within the scalar-relativistic calculations, Pt_7 clusters are planar in their ground state, with an atomic structure based on the square motifs and a total spin magnetic moment of 4 μ_B. Doping with a single iron impurity completely changes these trends. Spin excitations and chemical order compete in Pt_6Fe within the same energy window and a rich variety of isomers of different kinds is found. Three-dimensional structures are clearly favored over planar ones in Pt_6Fe clusters, and the total spin moment of the ground state (hexahedron plus two capping atoms) is larger by a factor two than that of Pt_7 in its ground state, and by a factor four compared with that of Pt_7 with the same three-dimensional structure. This increase of the total spin moment is large due to the local moment at the Fe site together with the induced increase of exchange splitting at the Pt atoms. Binding energies also increase in more than 100 meV/atom which means that the Fe impurity helps in stabilizing the nanoparticle besides increasing its total moment, both facts relevant from the technological point of view.

When the SOC is considered, the ground atomic state structures of Pt_7 and Pt_6Fe do not change, except for slight relaxations, although the SOC modifies the energetic order of the low-lying isomers in the pure Pt clusters. The orbital contribution to the total magnetic moment is comparable to the spin contribution, with noncollinear coupling between the local orbital and spin moments in many cases. The obtained values for the spin and orbital moments can be compared with future XMCD measurements. SOC leads to a mixing of the spin states of low-energy spin isomers obtained in the scalar-relativistic calculation. An inplane easy axis is found in the ground state of Pt_7, with a MAE of 40 meV, which means that its magnetic configuration is expected to be stable against magnetization reversal by thermal excitation at room temperature. In the iron-doped Pt_6Fe clusters, the MAE in the ground state (24 meV) is lower than that in Pt_7, but there exist certain metastable isomers with larger MAE than their pure counterparts having the same atomic structure. This trend is interesting since, for certain atomic configurations, doping with iron improves the quality of the magnetic nanoparticle in three aspects of technological relevance: increase of the total magnetic moment, of the MAE, and of the binding energy. Considering that magnetic grains are generally supported on substrates, such metastable configurations should be more feasible than in a free-standing environment.

Acknowledgments We acknowledge the support of the Spanish Ministry of Science and Innovation, the European Regional Development Fund, and Junta de Castilla y Leon (Grant Nos. FIS2011-22957 and VA104A11-2). P.G.A.L. acknowledges the financial support from CONACyT Ref. 165078, call 2011–2012 for sabbatical and postdoctoral positions for consolidation of research groups. F.A.G acknowledges the support from PROMEP-SEP-CA230, the Ministry of Education, Culture and Sport, Ref SAB2011-0024, Spain, and to the DIPC funds for a fellowship grant.

References

Aguilera-Granja F, Longo RC, Gallego LJ, Vega A (2010) Structural and magnetic properties of x12y (x, y=Fe, Co, Ni, Ru, Rh, Pd, and Pt) nanoalloys. J Chem Phys 132:184507

Apsel SE, Emmert J, Deng J, Bloomfield L (1996) Surface-enhanced magnetism in nickel clusters. Phys Rev Lett 76:1441–1444

Bader RFW (1990) Atoms in molecules. A quantum theory. Clarendon, Oxford

Billas IML, Châtelain A, de Heer WA (1994) Magnetism from the atom to the bulk in iron, cobalt, and nickel clusters. Science 265:1682–1684

Błoński P, Hafner J (2009) Magnetic anisotropy of transition-metal dimers: density functional calculations. Phys Rev B 79:224418

Błoński P, Hafner J (2011) Magneto-structural properties and magnetic anisotropy of small transition-metal clusters: a first-principles study. J Phys: Condens Matter 23:136001

Błoński P, Dennler S, Hafner J (2011) Strong spin–orbit effects in small Pt clusters: geometric structure, magnetic isomers and anisotropy. J Chem Phys 134:034107

Bucher JP, Douglass DC, Bloomfield LA (1991) Magnetic properties of free cobalt clusters. Phys Rev Lett 66:3052–3055

Castro M, Jamorski C, Salahub DR (1997) Structure, bonding, and magnetism of small Fe_n, Co_n, and Ni_n clusters, n 5. Chem Phys Lett 271:133–142

Diéguez O, Alemany MMG, C CR, Ordejón P, Gallego LJ (2001) Density-functional calculations of the structures, binding energies, and magnetic moments of fe clusters with 2 to 17 atoms. Phys Rev B 63:205407

Fernández-Seivane L, Ferrer J (2007) Magnetic anisotropies of late transition metal atomic clusters. Phys Rev Lett 99:183401

Fritsch D, Koepernik K, Richter M, Eschrig H (2008) Transition metal dimers as potential molecular magnets: a challenge to computational chemistry. J Comput Chem 29:2210–2219

García-Fuente A, Vega A, Aguilera-Granja F, Gallego LJ (2009) $Mo_{4x}fe_x$ nanoalloy: structural transition and electronic structure of interest in spintronics. Phys Rev B 79:184403

Hobbs D, Kresse G, Hafner J (2000) Fully unconstrained non-collinear magnetism within the projector augmented-wave method. Phys Rev B 62:11556–11570

Huda MN, Niranjan MK, Sahu BR, Kleinman L (2006) Effect of spin–orbit coupling on small platinum nanoclusters. Phys Rev A 73:053201

Knickelbein MB (2001) Experimental observation of superparamagnetism in manganese clusters. Phys Rev Lett 86:5255–5257

Kresse G, Furthmuller J (1996) Efficient iterative schemes for ab initio total-energy calculations using a plane-wave basis set. Phys Rev B 54:11169–11186

Kresse G, Hafner J (1993) Ab initio molecular dynamics for liquid metals. Phys Rev B 47:558–561

Kresse G, Lebacq O (2013) VASP Manual. http://cms.mpi.univie.ac.at/vasp/vasp/vasp.html

Kumar V, Kawazoe Y (2008) Evolution of atomic and electronic structure of pt clusters: Planar, layered, pyramidal, cage, cubic, and octahedral growth. Phys Rev B 77:205418

Marsman M, Hafner J (2002) Broken symmetries in the crystalline and magnetic structures of iron. Phys Rev B 66:224409

Meshcheryakov VF, Fetisov YK, Stashkevich AA (2008) Magnetic and microwave properties of nanocomposite films on the basis of FeCoNi particles of various shapes. J Appl Phys 104:063910

Montejano-Carrizales JM, Aguilera-Granja F, Morán-López JL (2011) Structural and magnetic properties of femyn (m + n=7, y = Ru, Rh, Pd, and Pt) nanoalloys. Eur Phys J D 64:53–62

Niemeyer M, Hirsch K, Zamudio-Bayer V, Langenberg A, Vogel M, Kossick M, Ebrecht C, Egashira K, Terasaki A, Moller T, v Issendorff B, Lau JT (2012) Spin coupling and orbital angular momentum quenching in free iron clusters. Phys Rev Lett 108:057201

Perdew JP, Burke K, Ernzerhof M (1996) Generalized gradient approximation made simple. Phys Rev Lett 77:3865–3868

Peredkov S, Neeb M, Eberhardt W, Meyer J, Tombers M, Kampschulte H, Niedner-Schatteburg G (2011) Spin and orbital magnetic moments of free nanoparticles. Phys Rev Lett 107:233401

Polak M, Rubinovich L (2004) Computational study of ternary alloy nanocluster compositional structures: NiCuRh versus NiCuPd. Int J Nanosci 3:625–630

Sahoo S, Hucht A, Gruner ME, Rollmann G, Entel P, Postnikov A, Ferrer J, Fernández-Seivane L, Richter M, Fritsch D, Sil S (2010) Magnetic properties of small Pt-capped Fe, Co, and Ni clusters: a density functional theory study. Phys Rev B 82:054418

Soler JM, Artacho E, Gale JD, García A, Junquera J, Ordejón P, Sánchez-Portal D (2002) The siesta method for ab initio order-n materials simulation. J Phys Condens Matter 14:2745

Sun S, Murray CB, Weller D, Folks I, Moser A (2000) Monodisperse FePt nanoparticles and ferromagnetic FePt nanocrystal superlattices. Science 287:1989–1992

Toneguzzo P, Viau G, Acher O, Vincent FF, Fiévet F (1998) Monodisperse ferromagnetic particles for microwave applications. Adv Mater 10:1032–1035

Vega A, Dorantes-Dávila J, Balbás LC, Pastor GM (1993) Calculated sp-electron and spd-hybridization effects on the magnetic properties of small Fe_n clusters. Phys Rev B 47:4742–4746

Zhen L, Gong YX, Jiang JT, Shao WZ (2008) Electromagnetic properties of FeNi alloy nanoparticles prepared by hydrogen-thermal reduction method. J Appl Phys 104:034312

Zitoun D, Respaud M, Fromen MC, Casanove MJ, Lecante P, Amiens C, Chaudret B (2002) Magnetic enhancement in nanoscale CoRh particles. Phys Rev Lett 89:037203